Acta Crystallographica Section B
Structural Science
ISSN 0108-7681

Structure of a synthetic halogen sulfosalt, $Cu_3Bi_2S_3I_3$

Tonči Balić-Žunić,[a]* Konstantin Mariolacos,[b] Karen Friese[c] and Emil Makovicky[a]

[a]Geological Institute, University of Copenhagen, Øster Voldgade 10, DK-1350 Copenhagen K, Denmark, [b]Beethoven Str. 38, D-37085 Göttingen, Germany, and [c]Departamento Física Materia Condensada, Facultad de Ciencia y Tecnología, Universidad del País Vasco, Apdo 644, 48080 Bilbao, Spain

Correspondence e-mail: tonci@geol.ku.dk

Received 21 June 2004
Accepted 16 March 2005

$Cu_3Bi_2S_3I_3$ was crystallized during an attempt to synthesize Cu–Pb–Bi sulfosalts with iodine as the transport medium. The crystal structure was solved from a black needle-like crystal on a four-circle diffractometer with a CCD detector. The solution was obtained by direct methods and subsequent difference-Fourier syntheses. S and I atoms are arranged in a systematically distorted cubic eutaxy (close packing). Bi atoms have monocapped trigonal prismatic coordinations, while Cu atoms occupy coordination sites which vary from trigonal planar to distorted tetrahedral. A prominent feature is the distribution of Cu atoms over many closely spaced sites in the structure, the majority of them being only partly occupied, which strengthens the case for mobile Cu atoms during crystal growth at elevated temperatures. In this respect, $Cu_3Bi_2S_3I_3$ represents an extreme example of a statistical distribution of Cu in the structure; a frequently observed property of this element in sulfosalts.

1. Introduction

With the exception of some mercury-dominated minerals (*e.g.* corderoite, kenhsuite, capgaronnite, perroudite), halogens play a minor role in those few naturally occurring sulfides known to contain them (*e.g.* the potassium or thallium iron sulfides bartonite, chlorbartonite, djerfisherite and thalfenisite, or the lead antimony sulfosalts dadsonite, pellouxite and pillaite). The atomic ratio of halogens to sulfur in the latter is below 1:25. In most of the compounds known it is chlorine that represents the halogens. However, a number of sulfo-halogenides relatively rich in various halogens have been synthesized and recently the first sulfo-iodide mineral, mutnovskite ($Pb_2AsS_3(I,Cl,Br)$), was found in the fumaroles of the Mutnovsky volcano on Kamchatka (Zelenski *et al.*, 2005). The specific conductive properties as semiconductors, ferroelectrics or ionic conductors make these compounds especially interesting.

Among the sulfo-iodides with known structure are BiSI (Haase-Wessel, 1973), $Bi(Bi_2S_3)_9I_3$ (Miehe & Kupčik, 1971) and $(Pb_{1-x},Bi_x)Bi_2Cu_2Cu_{2-x}S_5I_2$ (Ohmasa & Mariolacos, 1974). The present compound belongs to the same group, representing at the same time a unique structural type. It was synthesized during systematic work on the synthesis and crystal chemistry of sulfo-halogenides, which the second author conducted about 15 years ago. The two small crystals which remained from the synthesis which were used for the crystal structure determination were unfortunately lost during an attempt to prepare a sample for microprobe analysis. However, from the results of the crystal structure analysis, a satisfactory chemical composition of the compound could be determined.

doi:10.1107/S0108768105008530

Table 1
Experimental details.

Crystal data	
Chemical formula	$Bi_2Cu_{3.26}I_{2.62}S_{3.38}$
M_r	1065.97
Cell setting, space group	Monoclinic, *C*2/*m*
a, *b*, *c* (Å)	28.056 (6), 4.1048 (9), 10.580 (2)
β (°)	110.572 (4)
V (Å^3)	1140.7 (4)
Z	4
D_x (Mg m^{-3})	6.221
Radiation type	Mo *K*α
No. of reflections for cell parameters	1398
θ range (°)	6.0–32.3
μ (mm^{-1})	44.86
Temperature (K)	299 (2)
Crystal form, colour	Needle, black
Crystal size (mm)	1.0 × 0.04 × 0.02
Data collection	
Diffractometer	SMART 1000CCD, P4
Data collection method	φ and ω scans
Absorption correction	Gaussian
$T_{\min}$	0.291
$T_{\max}$	0.521
No. of measured, independent and observed reflections	5437, 2276, 1471
Criterion for observed reflections	$I > 2\sigma(I)$
$R_{\rm int}$	0.071
$\theta_{\max}$ (°)	33.7
Range of *h*, *k*, *l*	$-42 \Rightarrow h \Rightarrow 43$ $-4 \Rightarrow k \Rightarrow 6$ $-15 \Rightarrow l \Rightarrow 15$
Refinement	
Refinement on	F^2
$R[F^2 > 2\sigma(F^2)]$, $wR(F^2)$, S	0.049, 0.129, 0.89
No. of reflections	2276
No. of parameters	94
Weighting scheme	$w = 1/[\sigma^2(F_o^2) + (0.0719P)^2]$, where $P = (F_o^2 + 2F_c^2)/3$
$(\Delta/\sigma)_{\max}$	0.001
$\Delta\rho_{\max}$, $\Delta\rho_{\min}$ (e Å^{-3})	3.94, −4.59
Extinction method	*SHELXL*
Extinction coefficient	0.00022 (6)

Computer programs used: *SHELXS*97 (Sheldrick, 1997*a*), *SHELXL*97 (Sheldrick, 1997*b*).

2. Experimental

The crystals were synthesized from a mixture of the binary sulfides PbS, Bi_2S_3 and Cu_2S (2:1:1) with the addition of I_2, which served as a transport medium. The mass per free volume was 3 mg ml^{-1} inside an evacuated and sealed quartz glass tube of the dimensions 150 × 14 mm. The reaction proceeded for 2 weeks over a temperature gradient of 743–703 K. At the end of the experiment the quartz tube was quenched in running water.

The collection of the X-ray diffraction data and the crystal structure solution were carried out for both the available needle-shaped black crystals that remained from the synthesis. Somewhat better reliability factors were obtained for the smaller of the two crystals investigated, apparently because of the lower absorption and a more reliable correction. Its data are represented in Table 1.

SMART software was used to determine the crystal lattice orientation and data collection; *SAINT* software was used for the integration of intensities, *Lp* correction and calculation of the final unit-cell parameters. The parameters were determined from 1398 strong reflections with $I > 10\sigma(I)$ in the range $11.9 < 2\theta < 64.5°$. A Gaussian, face-indexed absorption correction of intensities was made by the program *XPREP*. All the programs used are Bruker-AXS products.

3. Structure solution

The crystal lattice has monoclinic geometry. The only observed systematic extinctions were due to the C centering. The structure was solved in the space group *C*2/*m* by direct methods (*SHELXS*97; Sheldrick, 1997*a*), which revealed the positions of Bi1, Bi2, I1, I2, I3, Cu1, Cu2*A*, S1, S2 and S3 (Fig. 1). The initial structure refinement was carried out using the program *SHELXL*97 (Sheldrick, 1997*b*). Subsequent difference-Fourier synthesis suggested a division of Bi2 in Bi2*A* and Bi2*B*. Furthermore, Cu4*A*, Cu4*B*, Cu4*C* and Cu2*B* in the neighbourhood of Cu2*A* were recognized, plus an additional Cu site (Cu5). All these sites were characterized by partial occupancies and were defined as Cu on the basis of their coordinations. In addition, the crystal chemical characteristics (stoichiometry, bond distances and a higher atomic displacement factor than the other two I sites) suggested that I3 is to be a mixed iodine–sulfur site. Finally, a residual maximum in the difference Fourier map was interpreted as an additional, partly occupied Cu site (Cu3).

In view of the complexity of the disorder phenomena in the structure, it was necessary to check the results by refining the anharmonic displacement parameters and therefore the program *JANA*2000 (Petříček & Dušek, 2000) was used.

With this program two different refinement strategies were followed simultaneously: in the first the non-ideal atomic sites were treated as split-atom positions as in the preliminary refinements, while in the second the Bi2, Cu4 and Cu2 positions were modelled as one position using anharmonic third-order displacement tensors.

Anharmonic treatment of the Bi2 and Cu2 positions leads to agreement factors which are comparable to those achieved in the corresponding split-atom models. However, for both positions the number of parameters is larger in the anharmonic model (12 compared with 9). For the Cu4 position, which is approximated by three distinct positions in the split-atom model, the number of parameters (12) is equal to the number assumed in an anharmonic model. However, in this case the agreement factors for the anharmonic model are significantly worse than for the split-atom model. Anharmonic refinement was therefore discarded and the split-atom model was finally accepted. The positions of the atoms used in this model were confirmed by the inspection of the joint probability density functions, taking into account the relevant atoms. The maxima from these functions do not differ significantly from the atomic positions obtained in any case.

In the final model all atomic positions, except Cu3, were refined with anisotropic displacement factors. The very close positions of Bi2*A* and Bi2*B*, I3 and S4, Cu2*A* and Cu2*B*, and Cu4*A*, Cu4*B* and Cu4*C* were constrained to have equal

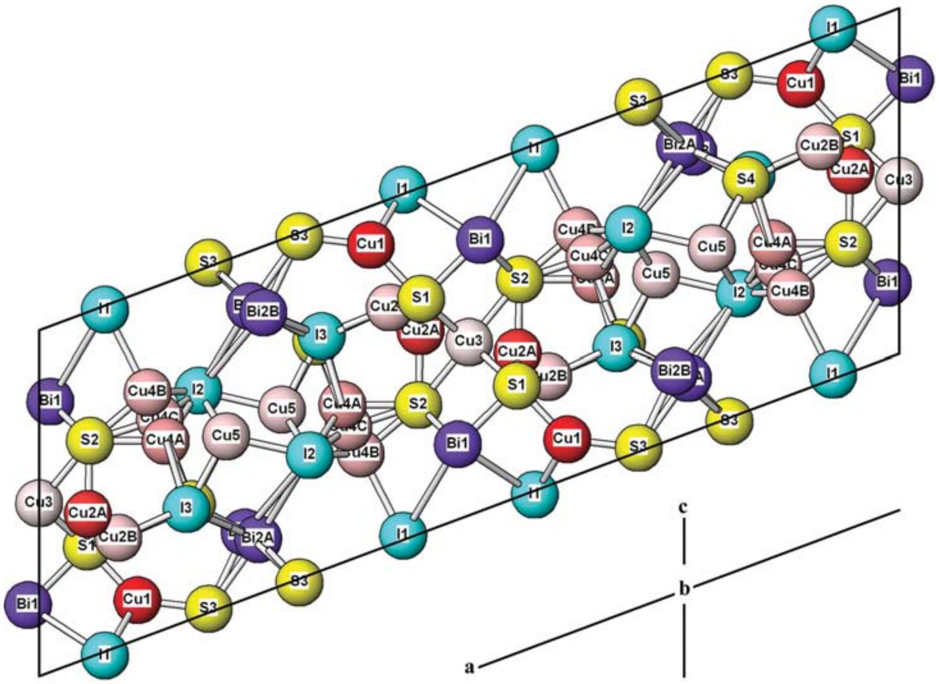

Figure 1
Projection of one unit cell of $Cu_3Bi_2S_3I_3$ parallel to the *b* axis with atom labelling. The intensity of colouring of the Cu atoms is proportional to the occupancy factor.

displacement factors, while the sum of their occupancies was constrained. The atomic coordinates and displacement parameters of I3 and S4 were also held equal because no significant difference in the positions was observed in the last stages of an unconstrained refinement. The partially occupied and non-split sites Cu3 and Cu5 were refined with free occupancy factors. At this stage the refinement showed very similar occupancies of I3 and Bi2*A* (0.63 and 0.67, respectively), and S4, Bi2B and Cu4*A* (0.37, 0.33 and 0.37, respectively), while the occupancy of Cu3 (0.09) was approximately half that of Cu2*B* (0.19). A simultaneous occupation of certain sites was impossible as it would result in interatomic distances which were too short, and at the same time the observed similarities in occupancies were due to crystal chemical reasons (see §6). Therefore, some additional constraints were introduced, and in the last refinement the full list of constraints was as follows:

Occupation factor [I3] = Occupation factor [Bi2*A*];

Occupation factor [S4] = Occupation factor [Cu4*A*] = Occupation factor [Bi2*B*] = 1 − Occupation factor [I3];

Occupation factor [Cu2*B*] = 1 − Occupation factor [Cu2*A*];

Occupation factor [Cu3] = 1/2 Occupation factor [Cu2*B*];

Occupation factor [Cu4*B*] + Occupation factor [Cu4*C*] = Occupation factor [I3].

The refinement was stopped when the changes in parameters became lower than 0.1 of their standard deviations. No parameter correlations larger than 0.9 were observed. The largest correlations between the positions and the anisotropic displacement factors were 0.79 for z[Bi2*A*]/U^{33}[Bi2*A*] and −0.75 for U^{33}[Bi2*B*]/z[Bi2*B*].

The final atomic parameters (coordinates, occupancies and equivalent isotropic displacement factors) have been deposited.[1]

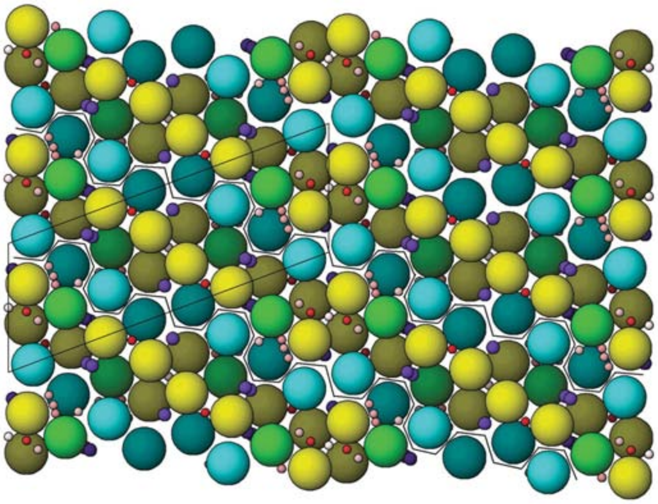

Figure 2
The close-packing of anions in the structure. Projection parallel to the *b* axis, with the *c* axis vertical. The outlines of a unit cell and the boundaries of one eutactic layer are marked. Anions are large and cations small. The colours of the atoms are as given in Fig. 1, except for the mixed S/I site which is drawn as a single green atom. Shading expresses depth along the projection direction.

4. Structure description

The anions (S and I atoms) are arranged in a cubic eutaxy ('close packing') periodically modified by crystallographic shear parallel to the $(117)_{cub}$ planes. In this way the structure is divided into four anionic row (I–S–S–I) broad layers (Fig. 2). The layers run parallel to $(\bar{2}01)$ of $Cu_3Bi_2S_3I_3$ and have step-like surfaces. The shear vector of the disturbed cubic eutaxy can be described as $\frac{1}{2}\mathbf{a} + \frac{1}{2}\mathbf{b} + 0\mathbf{c}$. In other words, the neighbouring $(117)_{cub}$ layers are mutually displaced by a $\frac{1}{2}\,[1\bar{1}0]_{cub}$ period (or $\frac{1}{2}$ [010] period of $Cu_3Bi_2S_3I_3$). The mutual displacement of neighbouring layers is obviously caused by the

---

[1] Supplementary data for this paper are available from the IUCr electronic archives (Reference: LC5011). Services for accessing these data are described at the back of the journal.

Table 2
Coordination parameters of Bi and Pb in sulfides and iodides.

The atomic coordinate parameters are defined in Balić-Žunić & Makovicky (1996) and Makovicky & Balić-Žunić (1998). All calculations were carried out using *IVTON* (Balić-Žunić & Vicković, 1996).

Compound	Coordination (Bi or Pb)	$d_{\min}$–$d_{\max}$ $\langle d \rangle$ (Å)	Polyhedron volume V_P (Å^3)	Sphere volume V_S (Å^3)	Volume distortion υ	Volume eccentricity Δ
$Bi_{6.333}S_9I$	8S	2.64–3.46 ⟨3.03⟩	48.2	116.6	0.045	0.450
$Cu_3Bi_3S_5I_2$	8S	2.66–3.47 ⟨3.07⟩	50.0	118.6	0.028	0.467
$Bi_{6.333}S_9I$	5S + 2I	2.60–2.94 ⟨2.80⟩ 3.57–3.60 ⟨3.58⟩	38.5	117.7	0.136	0.494
$Cu_3Bi_2S_3I_3$	5S + 2I (Bi2*B*)	2.58–3.04 ⟨2.85⟩ 3.71	41.2 (2)	127.8	0.148	0.532
BiSI	3S + 4I	2.59–2.74 ⟨2.69⟩ 3.20–3.74 ⟨3.47⟩	42.2	137.1	0.187	0.581
$Cu_3Bi_3S_5I_2$	3S + 4I	2.56–2.66 ⟨2.63⟩ 3.42–3.79 ⟨3.60⟩	44.6	134.6	0.124	0.606
$Cu_3Bi_2S_3I_3$	3S + 4I (Bi1)	2.56–2.66 ⟨2.63⟩ 3.48–3.85 ⟨3.67⟩	46.0 (2)	139.1	0.125	0.639
$Cu_3Bi_2S_3I_3$	3S + 4I (Bi2*A*)	2.62–2.73 ⟨2.70⟩ 3.14–3.64 ⟨3.39⟩	41.2 (2)	127.8	0.148	0.517
Bi_2S_3	7S	2.67–3.37 ⟨2.93⟩	35.9	105.6	0.101	0.359
		2.56–3.29 ⟨2.94⟩	35.5	107.2	0.126	0.406
PbS	6S	2.97	34.8	109.2	0	0
BiI_3	6I	3.05–3.12 ⟨3.08⟩	39.1	122.8	0.001	0.062
PbI_2	6I	3.23	44.8	140.8	0	0
$Pb_5S_2I_6$	3S + 5I	2.71–2.78 ⟨2.76⟩ 3.60–3.78 ⟨3.70⟩	64.6	162.8	0.085	0.533
$Pb_5S_2I_6$	1S + 6I	2.71 3.23–3.68 ⟨3.41⟩	51.2	157.1	0.139	0.380
$Pb_5S_2I_6$	6I	3.18–3.21 ⟨3.19⟩	43.3	136.2	0	0

necessity of allowing enough space for the lone-electron pairs of Bi atoms. In this way lone-electron-pair micelles are formed in the form of the trigonal prismatic voids between neighbouring layers (Fig. 3). The I atoms are concentrated along the planes of the crystallographic shear and participate in forming the trigonal prisms around the lone-electron pair micelles. The S atoms form the backbone of the layers, being involved in all the short Bi—X bonds.

In terms of the Bi and Cu coordination polyhedra, two different layers, traversing the shear planes, can be defined. The first (type *A*) is formed by capped trigonal coordination prisms of Bi, connected by single Cu coordination tetrahedra. They alternate with layers (type *B*) of a predominantly tetrahedral character formed by tetrahedral and triangular Cu coordinations, parallel to (001) (Fig. 3). The majority of Cu sites in the type *B* layers are only partially occupied. As they form a system of closely adjacent sites, a relatively easy diffusion of Cu parallel to (001) can be supposed in the present structure.

5. Related structures

The crystal structures of three other sulfo-iodides of bismuth are known, but have little resemblance to each other. In $Bi_{6.333}S_9I$ (Miehe & Kupčik, 1971), infinite $[Bi_4S_6]$ rods with the same configuration as in bismuthinite (Bi_2S_3) can be discerned. They form trigonal channels around trigonal axes which host I atoms. The rods are cyclically arranged around 6_3 axes with additional Bi atoms, which are disordered over the closely separated positions in hexagonal channels. This structure belongs to the zinkenite homologous series, a family of cyclically twinned rod-based sulfosalt structures (Makovicky, 1993). The same type of structure is also found in $Bi_{6.333}S_9Br$ (Mariolacos, 1976).

BiSI (Haase-Wessel, 1973) and its isotypes BiSCl, BiSBr, SbSBr, SbSI and SbSeI are related to BaI_2, $BaBr_2$ and $BaCl_2$ structures, which belong to the cotunnite-type ($PbCl_2$) structure (Sahl, 1963), built up of a tight network of tricapped trigonal prismatic coordinations of anions surrounding cations. Owing to the pronounced difference in the bond lengths of Bi—S and Bi—I, the coordination of Bi in BiSI is reduced to a monocapped trigonal prism with Bi residing in the capped prism face; arrangements of both anions and cations are more distorted than in the archetype structure. In analogy to Bi_2S_3, which contains $[Bi_4S_6]$ ribbons, BiSI can also be described as composed of double chains $[Bi_2S_2I_2]$.

The only other known bismuth sulfide–iodide structure which also contains Cu is $(Pb_{1-x}Bi_x)Bi_2Cu_2Cu_{2-x}S_5I_2$ or $Cu_3Bi_3S_5I_2$ (without minor Pb; Ohmasa & Mariolacos, 1974). There is a close connection between that structure and the structure of $Cu_3Bi_3S_3I_3$. The former can be completely reproduced by cutting out rods from the type A layers of the latter (Fig. 4*a*) and combining them in a new type of layers by overlapping four of the S sites (Fig. 4*b*). Such layers are combined in the structure of $Cu_3Bi_3S_5I_2$ by unit-cell twinning on mirror planes through one Bi and one S(I) site. As a consequence there is almost a full correspondence between the coordinations of Bi1, Cu1 and Cu2b and their interconnections in the present structure ($Cu_3Bi_2S_3I_3$), and those of Bi, Cu1 and Cu2 in $Cu_3Bi_3S_5I_2$, all of which belong to inner parts of the rods. The coordinations of Bi2 in the present structure and that of the (Bi, Pb) in $Cu_3Bi_3S_5I_2$, which are situated on rod peripheries, are different. The former are typical monocapped trigonal prisms paired with those from the neighbouring rod *via* the 2_1 axis, resulting in double columns of square coordination pyramids formed by the capped portions of trigonal prismatic coordinations. The latter are bicapped trigonal prisms, bisected by the mirror planes which also serve as the planes of the unit-cell twinning. $Cu_3Bi_2S_3I_3$ contains additional I and Cu sites situated in the type *B* layers (Fig. 4*a*).

6. Coordination characteristics of Bi and Cu

The quantitative coordination parameters calculated for Bi(Pb) and Cu sites in $Cu_3Bi_2S_3I_3$ and chemically related structures (Tables 2 and 3) are: the minimum ($d_{\rm min}$) and maximum ($d_{\rm max}$) bond distance, the average bond distance ($\langle d\rangle$), polyhedron volume (V_P), the volume of the sphere fitted to the positions of the coordinated atoms (V_S), volume distortion of the polyhedron (υ – calculated as a normalized volume difference to a polyhedron with the same coordination number and the maximum possible volume inscribed in the same sphere) and the volume eccentricity (Δ – calculated as a normalized volume difference between the fitted sphere and a sphere centered on the central atom and touching the former). The prerequisite for the calculation of the last three parameters is the determination of the centroid of coordination (Balić-Žunić & Makovicky, 1996).

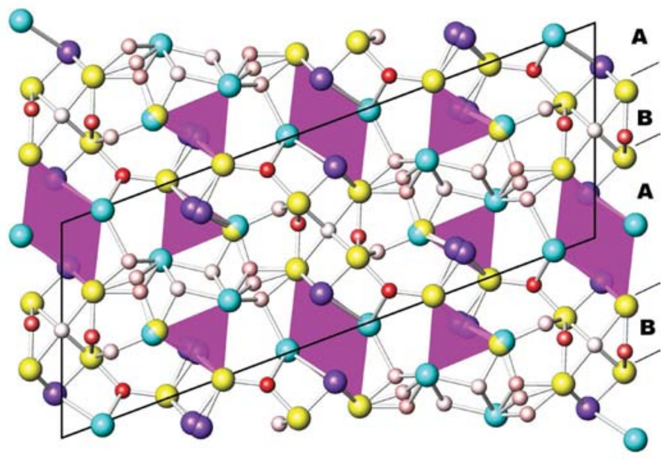

Figure 3
The lone-electron pair micelles of bismuth in the structure (purple). The colouring of the atoms is as given in Fig. 1. Projection parallel to the *b* axis. Layer types *A* and *B* are indicated.

The full coordinations of both independent Bi sites in $Cu_3Bi_2S_3I_3$ can be described as monocapped trigonal-prismatic or maybe better as split-octahedral coordinations, because Bi atoms are placed in the capped walls of the 'trigonal-prismatic' voids (Makovicky & Balić-Žunić, 1998; see Figs. 1 and 3). Partial substitution of S in the I3 site is obviously a reason for the splitting of the Bi2 site into the closely spaced Bi2*A* and Bi2*B*, the latter being occupied in the presence of S4. Inside the equivalent structural rods described above, the Bi2*A*/2*B* site in $Cu_3Bi_2S_3I_3$ corresponds to the Bi(Pb) site in $Cu_3Bi_3S_5I_2$, although the latter is coordinated only to S atoms owing to a different attachment of rods. The latter site is also split, but in this case owing to the requirements of accommodating both the short Bi—S bonds and the lone-pair of electrons in Bi inside a relatively large and symmetrically constrained coordination, which prevents Bi(Pb) taking a position in the centre of symmetry. In the case

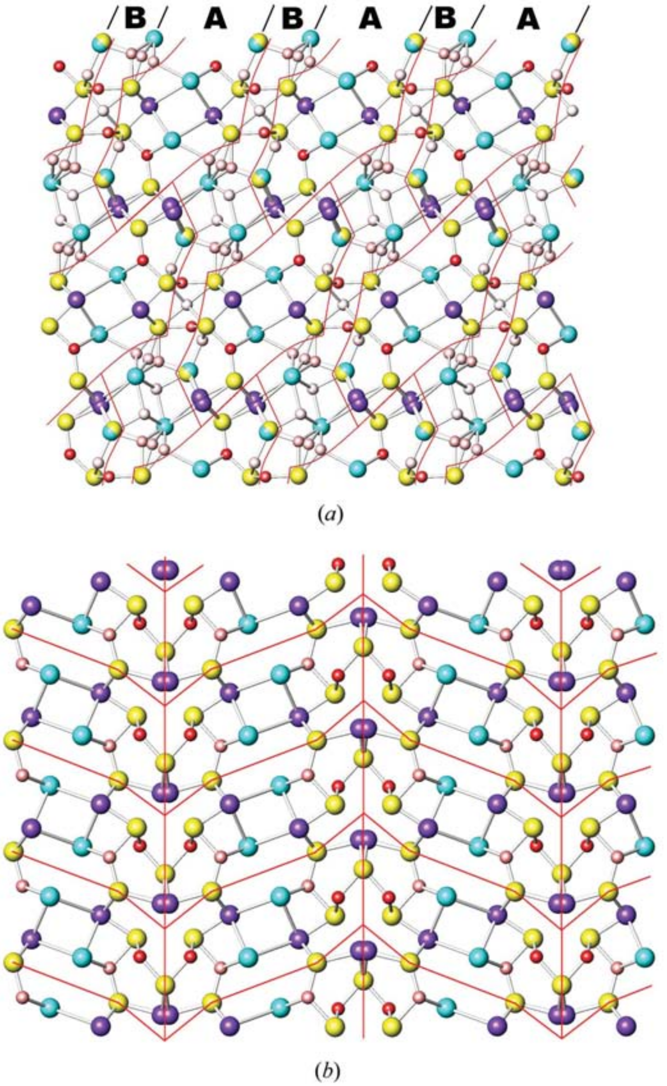

(*a*)

(*b*)

Figure 4
The crystal structures of (*a*) $Cu_3Bi_2S_3I_3$ (present work) and (*b*) $Cu_3Bi_3S_5I_2$ (Ohmasa & Mariolacos, 1974). The corresponding portions in the two structures are outlined in red. The colouring of the atoms is as given in Figs. 1–3.

Table 3
Coordination parameters for Cu sites in $Cu_3Bi_2S_3I_3$ and $Cu_3Bi_3S_5I_2$ (rows marked with an asterisk).

The atomic coordinate parameters are defined in Balić-Žunić & Makovicky (1996) and Makovicky & Balić-Žunić (1998). All calculations were carried out using *IVTON* (Balić-Žunić & Vicković, 1996).

Site	Coordination	$d_{\min}$–$d_{\max}$ $\langle d \rangle$ (Å)	V_P (Å^3)	V_S (Å^3)	υ	Δ
Cu1	2S + 2I	2.20–2.25 ⟨2.22⟩ 2.85	7.80 (8)	64.00	0.004	0.549
Cu2*A*	3S	2.25–2.28 ⟨2.27⟩	0	49.1	–	0.035
Cu2*B*	3S	2.28	0	49.5	–	0.104
Cu3	4S	2.52	6.67 (7)	67.1	0.189	0.006
Cu4*A*	2S + 2I	2.16–2.32 ⟨2.24⟩ 2.76	7.83 (8)	65.6	0.025	0.430
Cu4*B*	1S + 3I	2.29 2.58–2.82 ⟨2.66⟩	8.56 (9)	70.4	0.007	0.345
Cu4*C*	1S + 3I	2.23 2.52–2.87 ⟨2.64⟩	7.83 (8)	65.6	0.025	0.449
Cu5	4I	2.52–2.64 ⟨2.60⟩	8.87 (9)	73.5	0.014	0.100
Cu1*	3S	2.27–2.28 ⟨2.28⟩	0	47.3	–	0.448
Cu2*	2S + 2I	2.14–2.39 ⟨2.26⟩ 2.66	7.50	61.2	0.000	0.390

of $Cu_3Bi_3S_5I_2$ both the chemical analysis and the results of the crystal structure analysis suggest a partial substitution of Bi by Pb in this site (12% in the crystal for which the crystal structure was solved). As Pb was also present in the system during the synthesis of $Cu_3Bi_2S_3I_3$, the partial substitution of Bi by Pb can also be hypothesized for this compound. Comparison with the coordination parameters of various Bi and Pb coordinations in sulfides and iodides (Table 2) shows that only a minor substitution can be assumed in the present structure, because the differences compared with pure Bi coordinations are very small. The empirical formula $Cu_{3.27}Bi_2I_{2.64}S_{3.36}$ is not fully stoichiometric. Rather than a surplus of cation valence which would be expected in Pb for Bi substitution, it is very close to being balanced showing a small surplus (1%) of anion valence well inside the estimated uncertainty of the analysis method (X-ray diffraction). It is not expected that some of the copper is in a divalent state, which is not observed in other Cu–Bi sulfosalts and also not in $Cu_3Bi_3S_5I_2$ with a closely related structure and similar types of coordinations for the Cu atoms. However, due to a lack of accurate chemical analysis no definite conclusion about the complete absence of Pb in the structure can be made.

The Cu atoms occupy various tetrahedral and trigonal-planar voids of the anionic arrangement (Fig. 1). The fully occupied Cu1 site is tetrahedrally coordinated by two S and two I atoms, and connects (together with the partially occupied Cu2*B* site) the paired Bi1 coordinations with paired Bi2 coordinations inside the type *A* layers (Figs. 3 and 4*a*). The configuration of these two Cu sites, with a Cu—Cu separation of 2.87 Å, is equal to that found in $Cu_4Bi_4Se_9$ (Makovicky *et al.*, 2002). The trigonal-planar coordinated Cu2*A* and Cu2*B* atoms occupy two faces of a tetrahedral void formed by three S atoms and the mixed I3/S4 site. It is interesting to note that the coordinations of these two sites, especially that of Cu2*A*, differ from the equivalent Cu1 coordination in $Cu_3Bi_3S_5I_2$. Although all these sites are coordinated to three S atoms, in the latter case the Cu atom is significantly displaced from the plane of the S atoms, while the Cu2 sites in the present structure lie close to this plane, as evidenced by the eccentricity values (Δ) for these coordinations (Table 3). However, no significant differences in the Cu—S bond distances are observed. The displacement of Cu1 in $Cu_3Bi_3S_5I_2$ can be explained as the means of avoiding too close a contact between two fully occupied Cu1 sites across a mirror plane (Fig. 4*b*). In this configuration the centres of the coordinated S triangles are separated by only 2.34 Å, whereas the displaced Cu1 atoms become separated by 3.02 Å.

Cu3 is situated in the neighbourhood of the symmetry centre lying in the middle of an octahedral void formed by four S1 and two S2 atoms, and corresponds to one of the Cu coordination types found in pavonite homologues (Makovicky *et al.*, 2005). It statistically occupies both 'tetrahedral' halves of the void (but locally only one at a time) and cannot be present together with a neighbouring Cu2*A* site (Cu3—Cu2*A* 1.64 Å). The two Cu2*A* sites must therefore be vacated when Cu3 occupies the void and their counterparts, Cu2*B*, are occupied instead. The ratio of Cu3:Cu2*B* occupancies should therefore be 1:2. The Cu2*B*—I3/S4 distance is too short (2.28 Å) for a Cu—I bond (in CuI the bond distance is 2.62 Å; Wyckoff, 1963) and it can be concluded that the Cu2*B* site can only be occupied when S4 is present. This puts a limit on the maximum occupancy of both Cu2*B* and Cu3.

Cu4*A* has the same type of coordination as Cu1. It can be concluded that Cu4*A* is coordinated to S4 since the Cu4*A*—I3/S4 (2.18 Å) distance is once again too short for a Cu—I bond. Cu4*B* occupies the adjacent tetrahedral coordination, which shares a common face (2I2 + S2) with the coordination polyhedron of Cu4*A*. The short Cu4*A*—Cu4*B* distance (1.59 Å) shows that they cannot be occupied simultaneously. Cu4*C* is situated in the same tetrahedral void as Cu4*A* and it can be concluded that it is present when the mixed I/S site is occupied by iodine. The refinement resulted in similar occupancies for the three closely spaced Cu4 sites. Adjacent to them is the Cu5 site with 17% occupancy. As this site lies too close to the adjacent Cu4*A* and Cu4*C* sites (Cu—Cu distances are 1.86 and 2.1 Å, respectively), we conclude that it can be occupied only when an adjacent Cu4*B* site is occupied (2.75 Å apart). Cu5 is tetrahedrally coordinated by 4I.

7. Conclusions

The results suggest a statistical disorder for the majority of Cu atoms in the room-temperature structure. The partial occupancy of some sites, plus the splitting of one of the Bi sites, is caused by the substitution of S in one of the I sites, but the main reason for the spread of Cu over so many partially occupied sites must be the availability of many appropriate coordination sites in the structure, more than required by the stoichiometry of the compound. The proximity of the sites and their arrangement in continuous infinite layers point towards the mobility of Cu and ionic conduction at elevated temperatures.

Another potential property is the compositional variability resulting from the ability to incorporate Cu into different structure sites, combined with an S—I substitution. Assuming that the solid solution between S and I is concentrated only in the I3/S4 structural site, a potential solid-solution series can be envisaged along the $Cu_3Bi_2S_3I_3$–$Cu_4Bi_2S_4I_2$ line. The uppermost limit for the substitution of I by S on the I3/S4 site can be calculated from the crystallochemically determined occupancy relations described above. They can be summarized in the following equations (the site symbols represent the occupancies):

$$\begin{aligned}&\mathrm{Bi1} = \mathrm{I1} = \mathrm{I2} = \mathrm{Cu1} = \mathrm{S1} = \mathrm{S2} = \mathrm{S3} = 1\\ &\mathrm{Bi2}A = \mathrm{I3};\ \mathrm{Bi2}B = \mathrm{S4};\ \mathrm{I3} + \mathrm{S4} = 1\\ &\mathrm{Cu2}A = 1 - \mathrm{Cu2}B;\ \mathrm{Cu2}B \le \mathrm{S4}\\ &\mathrm{Cu3} = \tfrac{1}{2}\mathrm{Cu2}B;\ \mathrm{Cu3} \le \tfrac{1}{2}\mathrm{S4}.\end{aligned} \tag{1}$$

Additionally $\mathrm{Cu3} \le 0.5$ due to the exclusion of two neighbouring Cu3 sites.

$$\begin{aligned}&\mathrm{Cu4}A = \mathrm{S4};\ \mathrm{Cu4}B = 1 - \mathrm{Cu4}A - \mathrm{Cu4}C;\\ &\mathrm{Cu4}C = 1 - \mathrm{Cu4}A - \mathrm{Cu4}B\\ &\mathrm{Cu5} \le \mathrm{Cu4}B;\ \mathrm{Cu5} \le 1 - \mathrm{Cu4}A - \mathrm{Cu4}C;\\ &\mathrm{Cu5} \le 1 - \mathrm{S4} - \mathrm{Cu4}C\end{aligned} \tag{2}$$

$$\mathrm{Cu3} + \mathrm{Cu5} = \mathrm{S4} \quad \text{(requirement of stoichiometry).} \tag{3}$$

From the equations marked (1), (2) and (3) the following unequality/equality can be calculated

$$1.5\mathrm{S4} \le 1 - \mathrm{Cu4}C.$$

Assuming the possibility of a completely empty Cu4*C* site, this gives

$$\mathrm{S4} \le 2/3.$$

This defines $Cu_{3+2/3}Bi_2S_{3+2/3}I_{2+1/3}$ as the uppermost limit for the Cu + S ↔ I + □ substitution, with the following occupancies in the mixed or partly occupied sites

$$\begin{aligned}&\mathrm{Bi2}A = \mathrm{I3} = 1/3;\ \mathrm{Bi2}B = \mathrm{S4} = 2/3;\ \mathrm{Cu2}A = 1/3;\\ &\mathrm{Cu2}B = 2/3;\ \mathrm{Cu3} = 1/3;\ \mathrm{Cu4}A = 2/3;\ \mathrm{Cu4}B = 1/3;\\ &\mathrm{Cu4}C = 0;\ \mathrm{Cu5} = 1/3.\end{aligned}$$

The fact that the compositions of the investigated crystals were close to the middle of the presumed solid solution series can signify that these compositions at the same time enable the highest mobility (ionic conductivity) of Cu^+ at the temperature of synthesis (*ca* 720 K). The present crystal structure appears to be a picture of a frozen ionic conductor.

The X-ray diffraction analysis was supported by a grant from the Danish National Research Council (Natural Sciences), No. 21-03-0519. KF acknowledges financial support by the Spanish Ministerio de Ciencia y Tecnología.

References

Balić-Žunić, T. & Makovicky, E. (1996). *Acta Cryst.* B**52**, 78–81.

Balić-Žunić, T. & Vicković, I. (1996). *J. Appl. Cryst.* **29**, 305–306.

Haase-Wessel, W. (1973). *Naturwissenschaften*, **60**, 474.

Makovicky, E. (1993). *Eur. J. Mineral.* **5**, 545–591.

Makovicky, E. & Balić-Žunić, T. (1998). *Acta Cryst.* B**54**, 766–773.

Makovicky, E., Søtofte, I. & Karup-Møller, S. (2002). *Z. Kristallogr.* **217**, 597–604.

Makovicky, E., Søtofte, I. & Karup-Møller, S. (2005). Submitted for publication.

Mariolacos, K. (1976). *Acta Cryst.* B**32**, 1947–1949.

Miehe, G. & Kupčik, V. (1971). *Naturwissenschaften*, **58**, 219.

Ohmasa, M. & Mariolacos, K. (1974). *Acta Cryst.* B**30**, 2640–2643.

Petříček, V. & Dušek, M. (2000). *JANA*2000. Institute of Physics, Academy of Science of the Czech Republic, Praha, Czech Republic.

Sahl, K. (1963). *Beitr. Mineral. Petrogr.* **9**, 111–132.

Sheldrick, G. M. (1997*a*). *SHELXS*97. University of Göttingen, Germany.

Sheldrick, G. M. (1997*b*). *SHELXL*97. University of Göttingen, Germany.

Wyckoff, W. G. (1963). *Crystal Structures*, Vol. 1, pp. 108–111. New York: John Wiley and Sons.

Zelenski, M., Balic Zunic, T., Bindi, L., Garavelli, A., Makovicky, E., Pinto, D. & Vurro, F. (2005). Accepted for publication.